

Investigation of hydroxyapatite morphology at different experimental conditions

Ö. Dogan^{*}, B. Bodur

Yildiz Technical University, Chemical Engineering Department, Davutpasa Campus, 34210 Istanbul, Turkiye

Submitted: June 1, 2017; Accepted: September 1, 2017

The effects of experimental conditions and polymeric additives on hydroxyapatite (HAP) crystallization were investigated by wet chemical synthesis. Polyacrylic acid homopolymer and styrene-acrylic copolymer were used as additive. The obtained HAP powders were characterized by X-Ray Powder Diffraction (XRD), Scanning Electron Microscopy (SEM), Fourier Transform Infrared Spectroscopy (FTIR) and BET method. Thermal analysis (TG-DTA) was carried out to investigate the thermal stability of the powders. The result showed that the properties of HAP powders changed depending on the experimental conditions.

Keywords: Hydroxyapatite; polymeric additives; crystallization; chemical synthesis.

INTRODUCTION

Controlled synthesis of inorganic crystals is important on material fabrication which requires particles of specific size, shape and morphology. Experimental conditions and both organic and inorganic additives play an important role in crystallization process. They alter the surface properties of the crystals which have major effects on nucleation and growth which leads to change the shape and properties of the crystal [1].

The calcium phosphate salts is of particular interest because of its importance in various fields such as industrial water systems, wastewater treatment processes, agriculture fertilizers, biological calcification processes and drug delivery systems [2-5]. The thermodynamically most stable phase of calcium phosphate salt is hydroxyapatite (HAP, $\text{Ca}_5(\text{PO}_4)_3\text{OH}$). HAP properties depend on its stoichiometry and morphological characteristics especially its crystal size distribution, crystallinity, porosity and shape. Therefore recently, the study of controlling these parameters has gained great scientific and industrial interest. It was reported that small changes in these properties have significant effects on the mechanical properties of HAP crystals which are further processed to produce ceramics or incorporated with other materials to produce biocomposites [6-11].

In this study, the effects of temperature and polymeric additives on HAP crystallization were investigated by wet chemical synthesis. Polyacrylic acid homopolymer (PAA) and styrene-acrylic copolymer (SAA) were used as additive.

EXPERIMENTAL

Hydroxyapatite powders were prepared from calcium chloride and potassium dihydrogen

phosphate solution at specified temperature. During the crystallization process, the pH was kept constant in the range of 9-9.5 with additions of 0.1 M KOH solution. Nitrogen gas was introduced into the solution to ensure a CO_2 free atmosphere. In experiments where additives used, a similar procedure was followed and the polymer solutions were added to the reactant solutions. After the experiment was terminated, the precipitate was separated and then refluxed for twenty four hours in its supersaturated solution. At the end of this period, the powders were filtered, dried and stored in a desiccator.

Hydroxyapatite powders were sintered by thermal treatment with a heating rate of $10^\circ\text{C}/\text{min}$ for 3 hours at 650°C , 800°C and 1000°C . The obtained powders were characterized by X-Ray diffraction analysis (Phillips Panalytical X'ert Pro), FTIR spectral analysis (Bruker Alpha P), BET method (Quantachrome Instruments Autosorb 1), Scanning Electron Microscopy (JEOL-FEG-SEM) and thermal analysis (Perkin Elmer Pyris Diamond).

RESULTS AND DISCUSSION

X-ray diffraction analysis of the HAP powders was carried out by Phillips Panalytical X'ert Pro powder diffractometer. The data were collected in the 2θ range from 20 to 70° at scan rate of 0.020° step^{-1} . XRD pattern of the powders which synthesized at different temperature are shown in Figure 1. The grown main phase was identified as hydroxyapatite by XRD and compared with that of the JCPDS (01-073-0293) standards. As it can be seen from Figure 1, that the crystallinity of powders increases with the increase of synthesis temperature.

The specific surface area of the synthesized powders samples was determined by nitrogen

^{*}) To whom all correspondence should be sent:

E-mail: dogano@yildiz.edu.tr

sorption/desorption isotherms according to multiple point BET method. The powders were outgassed for 4 h at 40°C. The obtained specific surface areas and micropore volumes for non-sintered and sintered HAP powders are summarized in Table 1. As it can be clearly seen from Table 1, a decrease in synthesis

temperature results in an increase of the specific surface area, however reactant concentration does not effect the specific surface area. In addition, the increase in sintering temperature reduces the specific surface area.

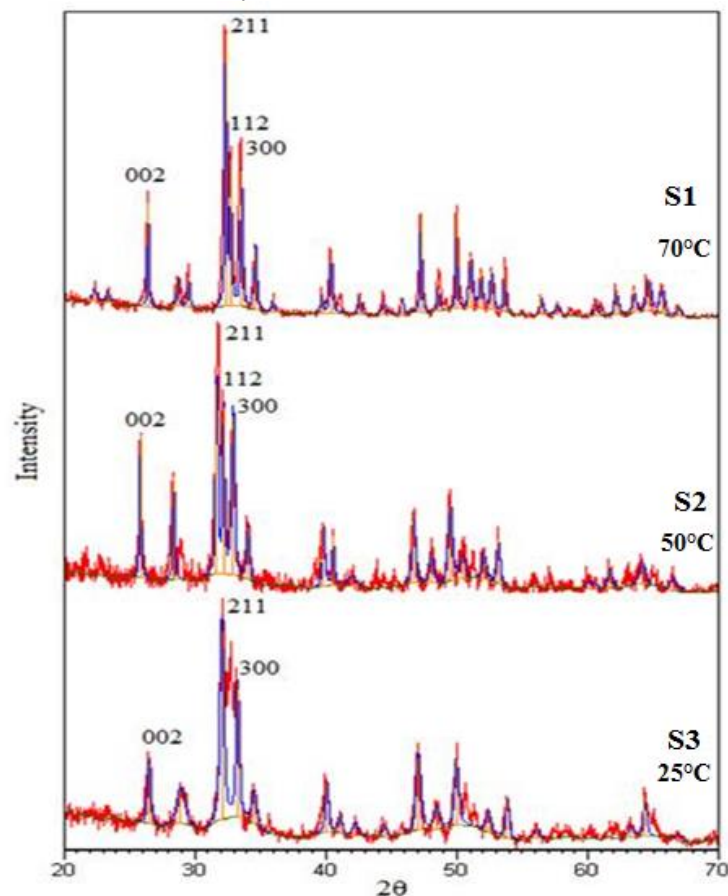


Figure 1. X-ray diffraction patterns of HAP powders synthesized at different temperatures.

Table 1. Effect of experimental conditions on the specific surface area of HAP powders.

Samples	T _{Ca} (mole/L)	Synthesis Temperature (°C)	Sintering Temperature (°C)	Specific Surface Area (m ² /g)	Micropore Volume (mm ³ /g)
S1	0.5	70	0	34.19	3.39
		70	650	23.04	1.42
		70	800	8.91	0.44
S2	0.5	50	0	62.25	4.49
		50	650	23.78	2.79
S3	0.5	25	0	80.30	7.75
		25	650	19.16	2.03
S4	1	70	0	36.18	2.54
		70	650	20.12	1.69
S5	0.25	70	0	32.11	1.55
		70	650	20.57	1.87

Purity of the samples was also tested by FTIR spectral analysis (Figure 2). FTIR spectra of the powders synthesized at 70°C showed that they consisted of HAP (S1). But FTIR spectra of the powders synthesized at 50°C (S2) and 25°C (S3),

showed a weak band at around 2300-2400 cm⁻¹, which was indicating that the dicalcium phosphate dihydrate (CaHPO₄·2H₂O) and the dicalcium phosphate anhydrite (CaHPO₄) are formed in the structure [12].

FTIR spectra of the powders synthesized at different reactant concentration are given in Figure 2. It showed a weak band at around 2300-2400 cm^{-1} for S3, S4 and S5 samples, which was indicating that

the dicalcium phosphate dihydrate ($\text{CaHPO}_4 \cdot 2\text{H}_2\text{O}$) and the dicalcium phosphate anhydrate (CaHPO_4) are formed in the structure [12].

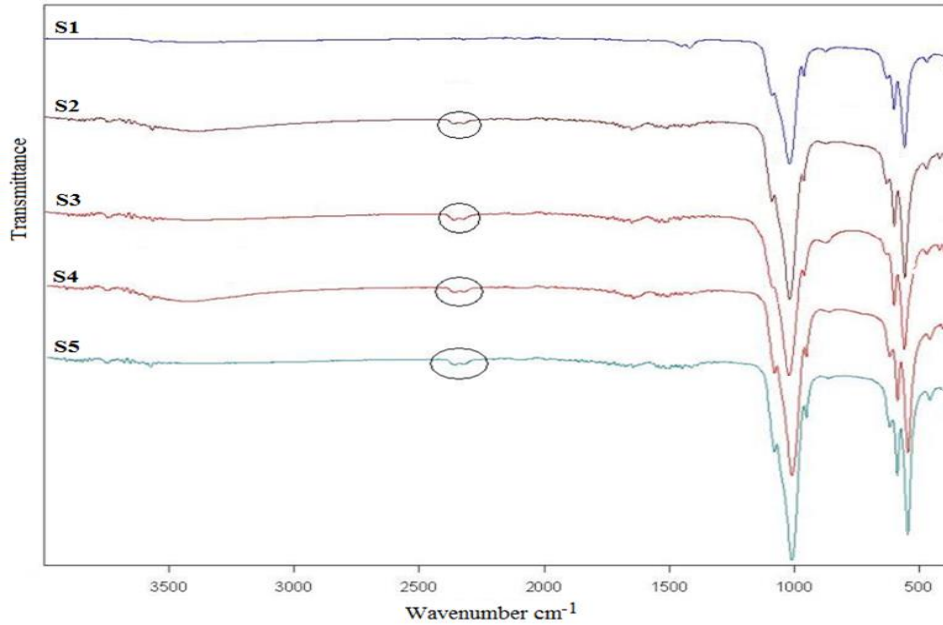


Figure 2. FTIR spectrums of HAP powders.

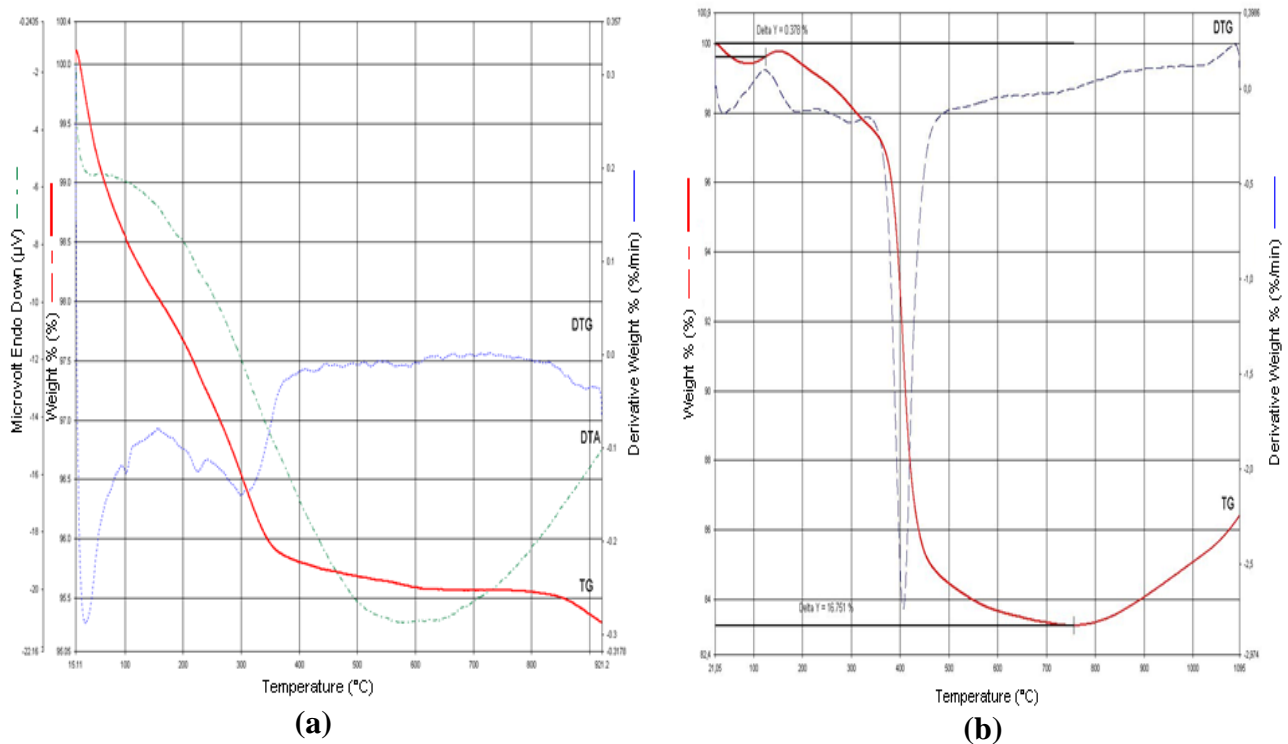


Figure 3. (a) TG, DTA and DTG curves for HAP powders synthesized without polymer addition (b) TG and DTG curves for HAP powders synthesized with polymer addition.

CO_3^{2-} ions were detected in the precipitate from the peaks around 1400 cm^{-1} . The presence of CO_3^{2-} ions indicates that the HAP formed during reaction includes some carbonate substituted apatite [7,13].

The stability phase composition of powders was analyzed by thermal treatment under nitrogen

atmosphere (Figure 3a). Initially, 2% weight loss was observed in sample due to moisture. TG analysis showed a two stage weight loss. The weight loss of about 1.1% was observed up to temperature 400°C, which is due to the evaporation of absorbed water from the surface and lattice water from the surface

and pores. Removal of the crystalline water may also take place in this temperature range. A continuous weight loss over 800°C is attributed to the loss of water from dehydroxylation of HAP [14,15]. The weight loss of 16.8% in the range of 120°C to 710°C temperature that can be seen from Figure 3b shows that the polymer is removed from the structure.

The obtained specific surface areas and micropore volumes for non-sintered and sintered HAP powders which are synthesized in the presence

of varying concentrations of polyacrylic acid homopolymer and styrene-acrylic copolymer are summarized in Table 2. It can be seen from Table 2, in the presence of styrene-acrylic copolymer, the specific surface area of powders does not change with increasing polymer concentration. However, in the presence of polyacrylic acid homopolymer, an increase in polymer concentration results in an increase of the specific surface area of the crystals.

Table 2. Effect of experimental conditions on the specific surface area of HAP powders in the presence of polymeric additives.

Samples	T _{Ca} (mole/L)	Polymer	Polymer Concentration (ppm)	Sintering Temperature (°C)	Specific Surface Area (m ² /g)	Micropore Volume (mm ³ /g)
S6	0.5	SAA	5000	0	30.31	...
	0.5	SAA	5000	650	17.43	1.52
	0.5	SAA	5000	800	11.68	1.46
S7	0.5	SAA	7500	0	31.32
	0.5	SAA	7500	650	23.81	2.63
S8	0.5	SAA	10000	0	29.93	...
	0.5	SAA	10000	650	22.79	2.39
	0.5	SAA	10000	800	13.53	1.15
	0.5	SAA	10000	1000	8.35	0.34
S9	0.5	SAA	15000	0	30.03	...
	0.5	SAA	15000	650	11.44	1.39
S10	0.5	PAA	2000	0	47.47	...
	0.5	PAA	2000	800	8.94	0.84
S11	0.5	PAA	5000	0	71.84	...
	0.5	PAA	5000	800	7.81	0.32
S12	0.5	PAA	10000	0	108.04	...

The crystal materials are usually sintered at high temperature to improve their mechanical properties, crystallinity and catalytic activity. Because of this understanding the sintering behavior of crystals that allows designing ceramics with controlled grain growth, microstructure and mechanical properties is important [16,17]. The FTIR spectrums of non-sintered and sintered powders synthesized in the presence 15000 ppm styrene-acrylic copolymer (S9) at different temperatures are given in Figure 4. The FTIR spectrum of the non-sintered powders showed the characteristic bands of HAP and styrene-acrylic copolymer. The FTIR spectrum of the powders sintered at 650°C showed that the peaks for styrene-acrylic copolymer around 760 cm⁻¹ disappears [18]. CO₃⁻² ions were detected in the precipitate from the peaks around 1400 cm⁻¹. At 1000°C sintering, the mode of the CO₃⁻² at 1400 cm⁻¹ group disappears in

all samples, which indicates an increase in crystallinity during sintering processes.

The morphologies of the HAP powders was analyzed by using SEM. The HAP powders synthesized at 70°C and sintered at 650°C are formed agglomerated particles of a needle-like morphology (Figure 5a). Figure 5b shows the SEM images of the HAP powders synthesized in the presence of 15000 ppm styrene-acrylic copolymer and sintered at 650°C. Significant changes in morphology were not observed in the presence of polymers. The precipitated crystals show similar needle-like shape. The powders precipitated at 70°C have average length of around 171 nm and width 55 nm. For the powders sintered at 650°C, the average length and width increased to 194 nm and 66 nm respectively. In the presence of 15000 ppm styrene-acrylic copolymer, the lengths and width of the crystals increased to 262 nm and 80 nm respectively.

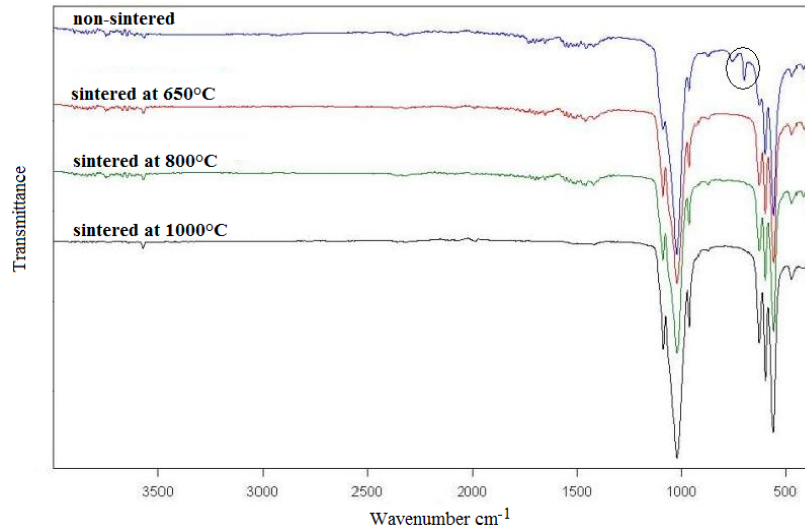


Figure 4. FTIR spectra of HAP powders synthesized in the presence of polymers.

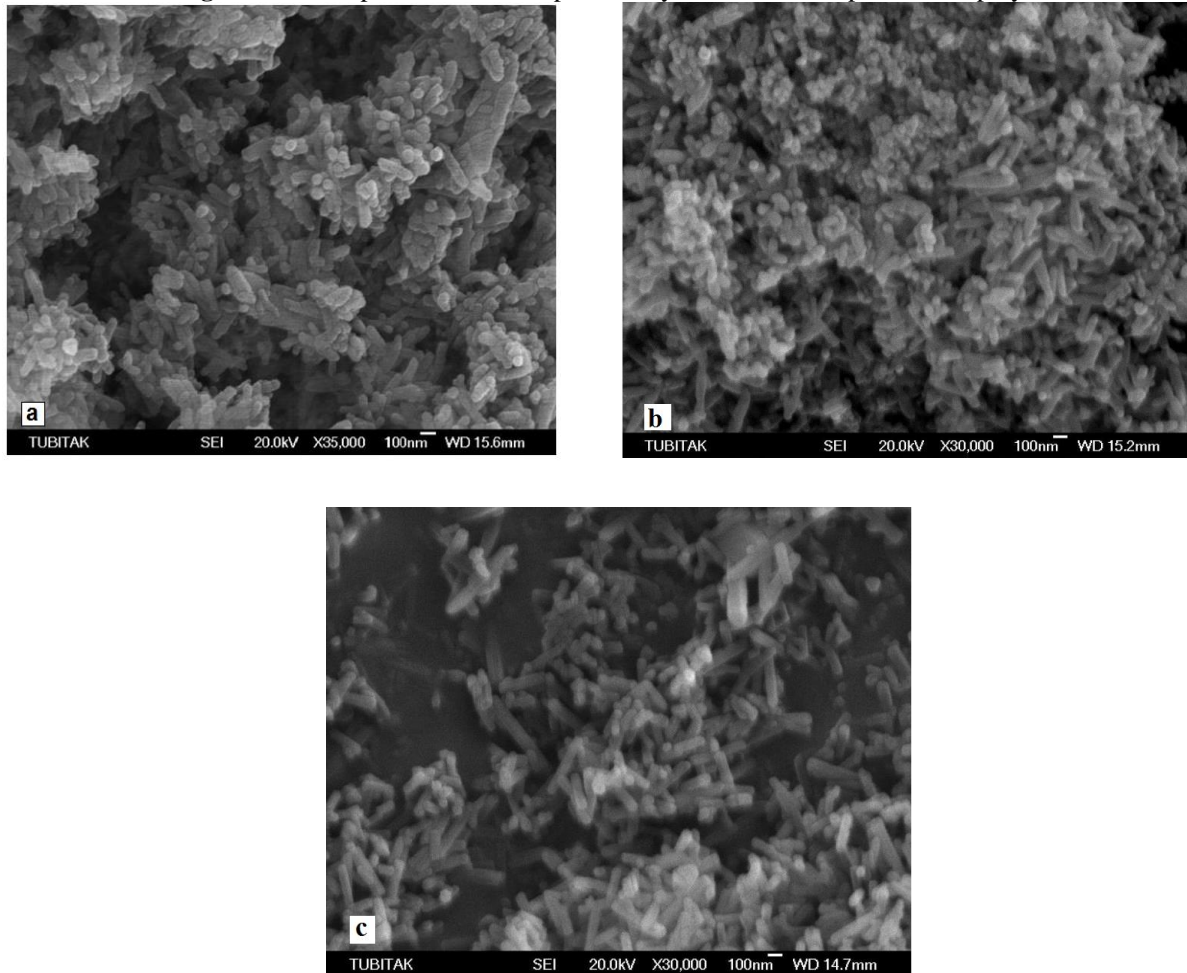


Figure 5. SEM of the HAP powders synthesized (a) without polymer addition and non-sintered (b) without polymer addition and sintered at 650°C (c) with polymer addition and sintered at 650°C.

CONCLUSIONS

The HAP powders were synthesized at different experimental conditions. Results show that the crystallinity, specific surface area, micropore volume and crystal size of the obtained powders changed depending on the experimental conditions. The specific surface area and the micropore volume

of powders increased with decreasing synthesis temperature while the crystallinity of crystals decreased. Sintering caused a decrease of the specific surface area and the micropore volume and an increase of the particle size and crystallinity. The particle size increased with addition of polymeric additives.

Acknowledgements. This study was supported by Yildiz Technical University Scientific Projects Coordination (project no: 2011-07-01-yulap02).

REFERENCES

1. M. Oner, O. Dogan, *Progress in Crystal Growth & Characterization of Materials*, **50**, 39 (2005).
2. B. Sandrine, N. Ange, B.A. Didier, C. Eric, S. Patrick, *J. Hazard. Mater. A*, **139**, 443 (2007).
3. H. H. Pham, P. Luo, F. Genin, A. K. Dash., *AAPS Pharm. Sci. Tech.*, **3**, 1 (2002).
4. H.-W. Kim, J. C. Knowles, H.-E. Kim, *Biomaterials*, **25**, 1279 (2004).
5. O. Dogan, M. Oner, *Langmuir*, **22**, 9671 (2006).
6. D. K. Son, Y. J. Kim, *Materials Sci. Eng. C*, **33**, 499 (2013).
7. P. Wang, C. Li, H. Gong, X. Jiang, H. Wang, K. Li, *Powder Technol.*, **203**, 315 (2010).
8. O. Dogan, M. Oner, *J. Nanosci. Nanotechnol.*, **8**, 667 (2008).
9. Y. X. Pang, X. Bao, *J. Eur. Ceramic Soc.*, **23**, 1697 (2003).
10. V.P. Orlovskii, V.S. Komlev, S.M. Barinov, *Inorganic Materials*, **38**, 973 (2002).
11. R. I. Martin, P. W. Brown, *J. Materials Science: Materials in Medicine*, **6**, 138 (1995).
12. S. Koutsopoulos, *J. Biomedical Mater. Res., Part A*, **62**, 600 (2002).
13. K. Agrawal, G. Singh, D. Puri, S. Prakash, *J. Minerals&Materials Character. Eng.*, **10**, 727 (2011).
14. Y. Chen, X. Miao, *Biomaterials*, **26**, 1205 (2005).
15. D. Malina, K. Biernat, A. Sobczak-Kupiec, *Acta. Biochim. Pol.*, **60**, 851 (2013).
16. N. Monmaturapoj, C. Yatongchai, *J. Metals, Materials & Minerals*, **20**, 53 (2010).
17. Y. C. Teh, C.Y. Tan, S. Ramesh, J. Purbolaksono, Y. M. Tan, H. Chandran, W. D. Teng, B. K. Yap, *Ceramics-Silikaty*, **58**, 320 (2014).
18. M.W. Urban, J.L. Koenig, L.B. Shih, J.R. Allaway, *Applied Spectroscopy*, **41**, 590 (1987).